



# Investigation of Gearbox Vibration Transmission Paths on Gear Condition Indicator Performance

*Paula J. Dempsey*  
*Glenn Research Center, Cleveland, Ohio*

*AKM Anwarul Islam*  
*Youngstown State University, Youngstown, Ohio*

*Jason Feldman and Chris Larsen*  
*Etegent Technologies, Ltd., Cincinnati, Ohio*

## NASA STI Program . . . in Profile

Since its founding, NASA has been dedicated to the advancement of aeronautics and space science. The NASA Scientific and Technical Information (STI) program plays a key part in helping NASA maintain this important role.

The NASA STI Program operates under the auspices of the Agency Chief Information Officer. It collects, organizes, provides for archiving, and disseminates NASA's STI. The NASA STI program provides access to the NASA Aeronautics and Space Database and its public interface, the NASA Technical Reports Server, thus providing one of the largest collections of aeronautical and space science STI in the world. Results are published in both non-NASA channels and by NASA in the NASA STI Report Series, which includes the following report types:

- **TECHNICAL PUBLICATION.** Reports of completed research or a major significant phase of research that present the results of NASA programs and include extensive data or theoretical analysis. Includes compilations of significant scientific and technical data and information deemed to be of continuing reference value. NASA counterpart of peer-reviewed formal professional papers but has less stringent limitations on manuscript length and extent of graphic presentations.
- **TECHNICAL MEMORANDUM.** Scientific and technical findings that are preliminary or of specialized interest, e.g., quick release reports, working papers, and bibliographies that contain minimal annotation. Does not contain extensive analysis.
- **CONTRACTOR REPORT.** Scientific and technical findings by NASA-sponsored contractors and grantees.

- **CONFERENCE PUBLICATION.** Collected papers from scientific and technical conferences, symposia, seminars, or other meetings sponsored or cosponsored by NASA.
- **SPECIAL PUBLICATION.** Scientific, technical, or historical information from NASA programs, projects, and missions, often concerned with subjects having substantial public interest.
- **TECHNICAL TRANSLATION.** English-language translations of foreign scientific and technical material pertinent to NASA's mission.

Specialized services also include creating custom thesauri, building customized databases, organizing and publishing research results.

For more information about the NASA STI program, see the following:

- Access the NASA STI program home page at <http://www.sti.nasa.gov>
- E-mail your question to [help@sti.nasa.gov](mailto:help@sti.nasa.gov)
- Fax your question to the NASA STI Information Desk at 443-757-5803
- Phone the NASA STI Information Desk at 443-757-5802
- Write to:  
STI Information Desk  
NASA Center for AeroSpace Information  
7115 Standard Drive  
Hanover, MD 21076-1320



# Investigation of Gearbox Vibration Transmission Paths on Gear Condition Indicator Performance

*Paula J. Dempsey*  
*Glenn Research Center, Cleveland, Ohio*

*AKM Anwarul Islam*  
*Youngstown State University, Youngstown, Ohio*

*Jason Feldman and Chris Larsen*  
*Etegent Technologies, Ltd., Cincinnati, Ohio*

National Aeronautics and  
Space Administration

Glenn Research Center  
Cleveland, Ohio 44135

Trade names and trademarks are used in this report for identification only. Their usage does not constitute an official endorsement, either expressed or implied, by the National Aeronautics and Space Administration.

*Level of Review:* This material has been technically reviewed by technical management.

Available from

NASA Center for Aerospace Information  
7115 Standard Drive  
Hanover, MD 21076-1320

National Technical Information Service  
5301 Shawnee Road  
Alexandria, VA 22312

Available electronically at <http://www.sti.nasa.gov>

# **Investigation of Gearbox Vibration Transmission Paths on Gear Condition Indicator Performance**

Paula J. Dempsey  
National Aeronautics and Space Administration  
Glenn Research Center  
Cleveland, Ohio 44135

AKM Anwarul Islam  
Youngstown State University  
Youngstown, Ohio 44555

Jason Feldman and Chris Larsen  
Etegent Technologies, Ltd.  
Cincinnati, Ohio 45212

## **Abstract**

Helicopter health monitoring systems use vibration signatures generated from damaged components to identify transmission faults. For damaged gears, these signatures relate to changes in dynamics due to the meshing of the damaged tooth. These signatures, referred to as condition indicators (CI), can perform differently when measured on different systems, such as a component test rig, or a full-scale transmission test stand, or an aircraft. These differences can result from dissimilarities in systems design and environment under dynamic operating conditions. The static structure can also filter the response between the vibration source and the accelerometer, when the accelerometer is installed on the housing.

To assess the utility of static vibration transfer paths for predicting gear CI performance, measurements were taken on the NASA Glenn Spiral Bevel Gear Fatigue Test Rig. The vibration measurements were taken to determine the effect of torque, accelerometer location and gearbox design on accelerometer response. Measurements were taken at the housing and compared while impacting the gear set near mesh. These impacts were made at gear mesh to simulate gear meshing dynamics. Data measured on a helicopter gearbox installed in a static fixture were also compared to the test rig. The behavior of the structure under static conditions was also compared to CI values calculated under dynamic conditions. Results indicate that static vibration transfer path measurements can provide some insight into spiral bevel gear CI performance by identifying structural characteristics unique to each system that can affect specific CI response.

## **Introduction**

Helicopter transmission health is important to helicopter safety because helicopters depend on the power train for propulsion lift and flight maneuvering. Health and Usage Monitoring Systems (HUMS) capable of predicting impending transmission component failure for “on-condition” maintenance have the potential to decrease operating and maintenance costs, and increase safety and aircraft availability. “On-condition” maintenance refers to maintenance when HUMS “condition indicators” indicate decreased performance, instead of relying on time-based maintenance intervals. These HUMS “condition indicators” (CI) are typically vibration signatures generated from fault patterns produced when damaged components interact with their environment. For gear CIs, these signatures relate to changes in dynamics at the gear mesh due to tooth damage.

Condition indicators can perform differently when measured on a component test rig or a full-scale transmission test stand or an aircraft. Damage progression tests are being performed in the Spiral Bevel Gear Fatigue Test Rig, as shown in Figure 1, at NASA Glenn Research Center (GRC). The objective of

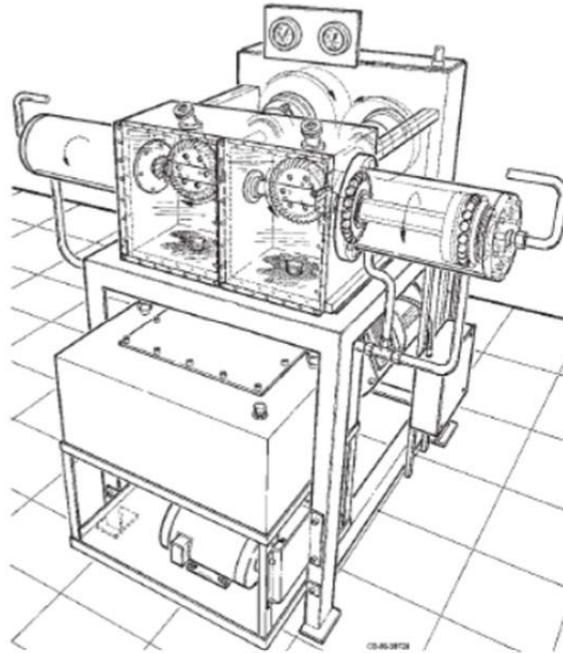


Figure 1.—Spiral bevel gear fatigue test rig at NASA GRC.



Figure 2.—Three spiral bevel geared systems.

these tests, as outlined in Reference 1, are to determine if ‘seeded or accelerated fault’ tests, in which a component is tested with a known fault, can be used as evidence that a HUMS condition indicator will reliably detect tooth damage when installed on a helicopter. Performing these tests will also identify limitations using seeded fault test rig data to demonstrate helicopter CI performance. For this approach, existing in-service HUMS flight data from spiral bevel gears installed in a helicopter nose gearbox (NGB) will be compared to test rig spiral bevel gear failure progression data. The field data analysis of spiral bevel gears condition indicators determined the CIs that performed the best in the field. The information learned from this analysis, documented in References 2 and 3, was fed into the development of the spiral bevel gear rig test plan.

In addition to performing dynamic tests of gears with varying levels of damage to gear teeth, measurements were taken to characterize differences in structural dynamics between the helicopter and test rig gearboxes. Although the transfer path can change under dynamic conditions due to load and speed, the static structure also filters the response between the vibration source and the accelerometer on the housing. Understanding structural differences between systems may provide insight into the difference in performance of diagnostic tools between such systems.

The approach used to assess the effectiveness of vibration transfer paths in predicting CI performance was to compare measurements on three spiral bevel geared systems. These three systems, as shown in Figure 2, are a helicopter NGB, an NGB fixture (an NGB removed from a helicopter and installed in a static fixture), and a test rig (spiral bevel gear fatigue test rig). The latter two are installed at NASA GRC.

This comparison required taking measurements on the helicopter NGB or NGB fixture that can be compared to future measurements on the test rig. Limited accessibility to the gear mesh within the helicopter NGB made it impossible to simulate an impact of gear teeth at the source, directly between meshing gear teeth. However, the NGB fixture enabled the application of impacts close to the gear mesh with varying torques—common during aircraft operations. Results from comparisons of frequency response functions between the helicopter NGB and NGB fixture under similar conditions found both systems to be consistent. These results are detailed in Reference 4. To determine if transfer path measurements under static conditions can provide insight into the gear CI performance during operation, measurements under dynamic conditions were required.

The objective of this paper was to assess the utility of vibration transfer paths of the test rig in a static condition for predicting its gear CI performance during its operation. The focus was on the the signal transmission from the gear mesh inside the gear box to the accelerometer installed on the gearbox external housing.

Measurements were taken on the static test rig to determine the effect of torque, accelerometer location and gearbox design on the accelerometer response to impacts near the gear mesh. Impacts of the gear set near mesh were made to simulate gear meshing dynamics. Data measured on the the NGB fixture, per Reference 4, were also compared to those of the test rig. Inferences were made comparing vibration measurements of the structure collected under static conditions to CI values calculated under dynamic conditions.

## Test Facility

Tests were performed in the test rig at NASA GRC. A detailed description of this test facility, as illustrated in Figure 1, can be found in References 5 and 6. In addition to developing gear health monitoring tools, the test facility has been used to study the effects of gear material, gear tooth design, and lubrication on the fatigue strength of gears. Two sets of spiral bevel gears are installed in the test rig and tested simultaneously. Facing the gearboxes per Figure 1, the left gear set (pinion/gear) is referenced as ‘left’ and the right gear set (pinion/gear) is referenced as ‘right’ within this paper.

Figure 3 shows the cross-sectional view of the test rig. The facility operates in a closed-loop arrangement where the load is locked into the loop via a split shaft and a thrust piston on the slave side of the rig. This forces a helical gear into mesh per Figure 3. The rotation is obtained using a drive motor connected through v-belts to the helical gear. The spiral bevel gears on the left side operate where the pinion drives the gear. The right side of the facility acts as a speed increaser where the gear drives the

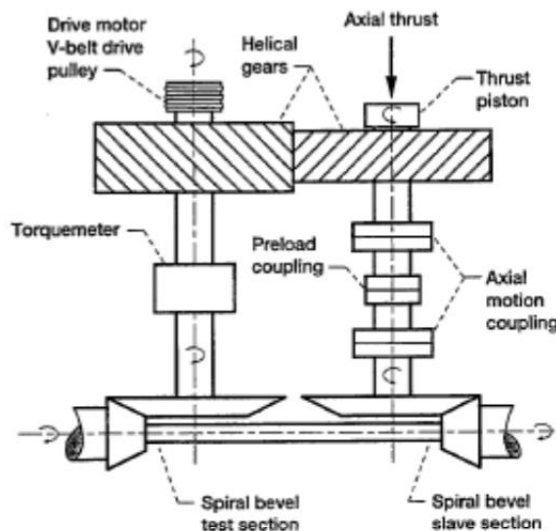


Figure 3.—Cross-section of the test rig.

pinion. The concave side of the pinion is always in contact with the convex side of the gear on both the left and right side of the gearbox. Load and speed are monitored by torque and speed sensors. The 41-tooth gear and 19-tooth pinion gear set are typically tested at a gear speed of 3500 rpm and a pinion speed of 7553 rpm with a gear torque of approximately 8000 in.-lb and a pinion torque of 3707 in.-lb.

Turbine engine oil that meets DOD-L-87354 specifications is used in the test rig. Both gear sets are lubricated with oil jets pumped from an oil reservoir. The lubrication exits the gearbox, and flows through an inductance type in-line oil debris (OD) sensor and then a magnetic chip detector. A strainer and a three-micron filter are located downstream of the OD sensor to capture any debris before returning to the sensor and the gearbox.

## Data Acquisition and Instrumentation for Dynamic Tests

During dynamic tests, three data acquisition systems were used. Vibration, oil debris, torque and speed data were collected once every minute with the NASA GRC data acquisition system, referred to as the Mechanical Diagnostic System Software (MDSS). Vibration and speed data were collected from a second set of sensors with a helicopter HUMS referred to as the Modern Signal Processing Unit (MSPU). Operational parameters were collected with a third system referred to as the Daytronic. These operational parameters included torque, speed, right and left gearbox oil inlet, and outlet temperatures and pressures.

A non-contact rotary transformer shaft-mounted torque sensor was used to measure torques during testing. Thermocouples were used to measure inlet and outlet oil temperatures. The inductance type OD sensor was used to measure the debris generated during fatigue damage to the gear teeth. Also measured were chip indications from the chip detector, when the gap was closed with debris.

For the MDSS system, accelerometers, with a frequency range of 0.7 to 20 kHz and a resonant frequency of  $\geq 70$  kHz, were installed on the right and left side of the test rig housing. These accelerometers were referred to as high frequency (HF) accelerometers in the analysis that follows. The MDSS HF accelerometers were mounted on the housing, radially and vertically with respect to the pinion, as shown in Figure 4. This orientation was chosen because the calculated forces at the mesh indicated the accelerometer would see the largest forces in this orientation. Speed is measured with optical tachometers mounted on the left pinion shaft and left gear shaft to produce a separate once-per-rev tachometer (tach) pulse for the pinion and gears.

For the MSPU system, accelerometers, with a frequency range of 0.5 to 5 kHz and a resonant frequency of 26 kHz, are also installed on the right and left side of the test rig. These accelerometers are referred to as the Dytran in the analysis that follows. A magnetic tachometer is installed on the right pinion to measure pinion pulses per tooth pass in the MSPU system. The accelerometers were mounted on the housing, in close proximity to the MDSS accelerometers, radially and vertically with respect to the pinion, as shown in Figure 4.

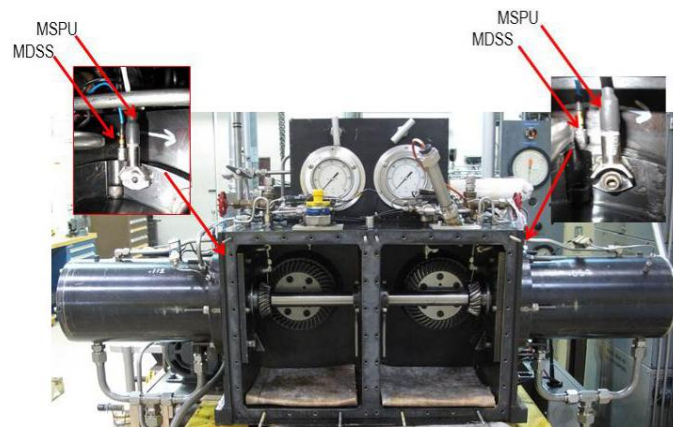


Figure 4.—Locations of accelerometers.

## Condition Indicator Analysis

For condition indicator calculations, vibration data were collected for the right and left pinion/gear sets using accelerometers mounted on the right and left side of the test rig gearbox per Figure 4. Data were collected at sample rates that provided sufficient vibration data for calculating time synchronous averaged (TSA) data. The TSA refers to techniques for averaging vibration signals over several revolutions of the shaft, in the time domain, to improve signal-to-noise ratio (Ref. 7). Using a once per revolution signal, the vibration signal is interpolated into a fixed number of points per shaft revolution. Signals synchronous with the shaft speed will intensify relative to the non-periodic signals.

Since helicopter gears generate vibration signals synchronous with speed, all helicopter gear condition indicators are calculated from TSA data. Gear vibration condition indicators are indexes calculated from vibration signal information. Many are based on statistical measurements of vibration energy. Signal processing techniques used to calculate a gear CI from the TSA vibration signal are discussed in detail in Reference 8. Some gear CI's are calculated directly from the time domain TSA signal, such as the root mean square (RMS), while others are calculated from the TSA converted to the frequency domain, such as the Sideband Index (SI).

Time synchronous averaging of the vibration data collected from the left and right accelerometer is performed in the MDSS system for pinions via the pinion tach pulse and for gears via the gear tach pulse. The MSPU system uses the magnetic tachometer installed at the pinion to calculate the TSA for both the pinion and the gear. The gear ratio is used to process the pinion data at the correct speed for the gear. Note that accelerometers installed on the left side of the test rig were used to measure vibration and calculate CIs for the pinion and gear installed on the left side of the gearbox. Accelerometers installed on the right side of the gearbox were used to measure vibration and calculate CIs for the pinion and gear installed on the right side of the gearbox.

Figure 5 illustrates the information used to calculate the TSA for the right gear and pinion. Using the sample rate of 200 kHz for one second duration and the speed of both shafts, the number of TSA averages for each acquisition is determined. Each average consists of one revolution of the shaft. Each average is made up of the number of linearly interpolated points rounded down to a power of two. A power of two

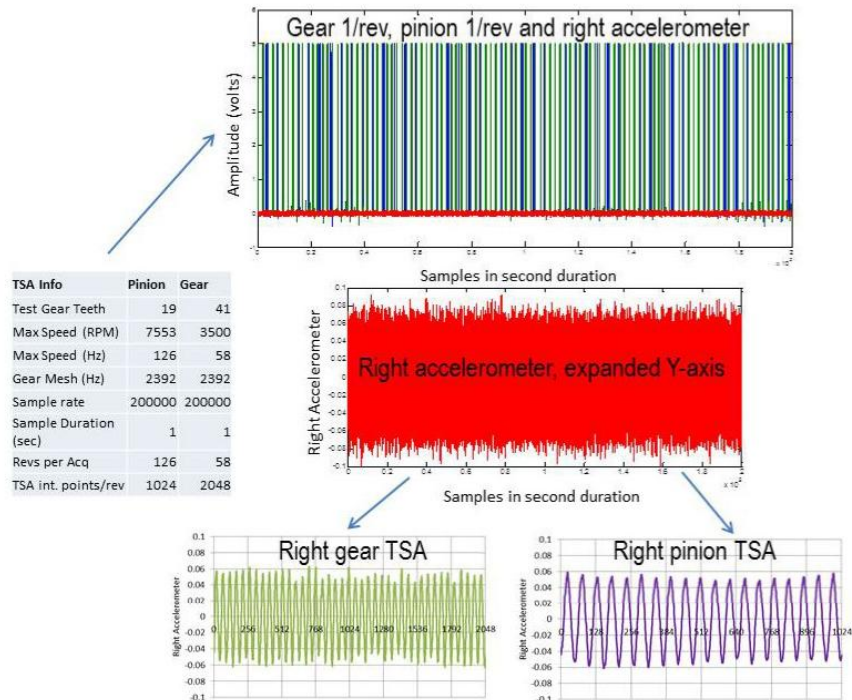


Figure 5.—Information used to calculate TSA.

data points is required to perform the Fast Fourier Transform (FFT) to convert time domain signals into the frequency domain. According to Figure 5, the top plot displays the right accelerometer data sampled for one second at 200 kHz. The green and blue lines are pulses from the gear and pinion 1/rev signal measured for each shaft rotation during this one second period. Only the right accelerometer is plotted in red in the middle plot with an expanded y-axis scale. The two lowest plots are the TSA signals calculated from the 1/rev and vibration data for the right gear and pinion. Pulses from the 41-tooth gear and the 19-tooth pinion can easily be seen within these two plots.

The SI methods were studied in this work for use in detecting surface fatigue damage to spiral bevel gear teeth. These methods were selected for use in this study due to the success at detecting damage to spiral bevel gear teeth in several helicopters (Refs. 2 and 3). The SI is a frequency domain based CI. The CI value is an average value of sideband amplitudes about the fundamental gear mesh (GM) frequency. The number of sidebands included in the calculation of the sideband CI can vary with different health monitoring systems.

All gears generate a dominant GM frequency in the vibration signature due to each tooth impacting against the gear it is driving as the teeth mesh. The gear (or pinion) mesh frequency is equal to the number of teeth multiplied by its speed. Gear sets also produce pairs of equally spaced sidebands on either side of the gear mesh. The sidebands are the frequencies calculated as the total number of gear teeth plus n and minus n (where n is an integer) multiplied by the gear speed in Hz. Certain types of gear tooth damage, such as pitting on several teeth, can affect the amplitude of sidebands. Increases in sideband amplitudes are often used to calculate a gear condition indicator. Table 1 lists the gear frequencies and the first order sideband frequencies for the tested pinion and gear at its operating speed.

Figure 6 illustrates the steps required to calculate RMS and SI for each reading. The RMS method uses the interpolated TSA data per Figure 5 to calculate the RMS of the TSA. The SI method uses the TSA data in performing the FFT. Then the peak amplitudes of the FFT data on either side of the GM are used to calculate SI indexes. Note that the x-axis of the plot showing the FFT of the right gear is in shaft orders or multiples of shaft speed. For example, since the gear has 41 teeth, the gear mesh frequency (teeth x speed) shows up at 41 shaft orders.

TABLE 1.—SIDE BAND FREQUENCIES

Gear			Sideband frequencies (Hz)						
No. teeth	Speed (rpm)	Speed (Hz)	38	39	40	GM	42	43	44
41	3500	58	2217	2275	2333	2392	2450	2508	2567
Pinion			Sideband frequencies (Hz)						
No. teeth	Speed (rpm)	Speed (Hz)	16	17	18	GM	20	21	22
19	7553	126	2014	2140	2266	2392	2518	2643	2769

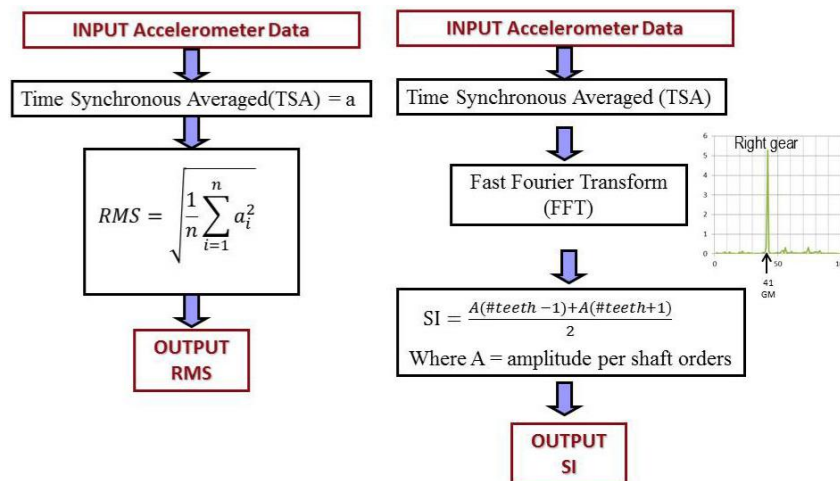


Figure 6.—RMS and SI calculations.

## Data Acquisition for Transfer Path Measurements

Modal analysis is primarily concerned with resonant frequencies or natural frequencies of a structure. It is typically performed by exciting a structure with a known force and measuring the vibration response at various locations on the structure. Frequency response functions (FRF) are used to analyze structural dynamics under static conditions and to estimate modal parameters for the analysis of mechanical systems. The FRF is used to measure the input-output relationship between two points on a structure as a function of frequency. Coherence is used to measure the linear dependence between the output and input signals as a function of frequency.

Vibration transfer path (VTP) measurements were recorded on the test rig at NASA GRC from June 3 to June 7, 2013. The objective of this effort was to perceive how an accelerometer responds to the impacts at the gear mesh as they travel through the structure. Since the structure filters this response, it can impact a CI's ability to detect tooth damage at the mesh. The transmission or transfer path of the test rig gearbox was determined by applying an impact force at the mesh and measuring its response with accelerometers installed on the gearbox housing. The same MDSS and MSPU accelerometers used for dynamic measurements were used for VTP measurements on the test rig, as shown in Figure 4.

Since the purpose of these tests was to determine the effect of the structure on the gear CI, the FRFs focused on the frequency ranges used for gear CI sideband index. Most of the FRF measurements were made with an instrumented impact hammer. The hammer provides good excitation up to 6400 Hz. For some test conditions, a commercial reaction-mass shaker in the form of a piezoelectric actuator was used.

The Kolmogorov–Smirnov test (K-S test) was used to compare the FRFs under different conditions. The KS test is a nonparametric test for the equality of continuous, one-dimensional probability distributions that can be used to compare two samples. The KS statistic quantifies a distance between the empirical cumulative distribution functions (CDF) of two samples. The two-sample KS test is one of the most useful and general nonparametric methods for comparing two samples, as it is sensitive to differences in both location and shape of the CDF of the two samples (Ref. 9). The Kolmogorov-Smirnov statistic  $D_{n,n'}$  is defined by Equations (1) and (2).

$$D_{n,n'} = \sup_x |F_{1,n}(x) - F_{2,n'}(x)| \quad (1)$$

$$F_n(x) = \frac{1}{n} \sum_{i=1}^n I[X_i \leq x] \quad (2)$$

Where,  $\sup_x$  is the supremum (greatest) distance between the empirical distribution functions  $F_{1,n}$  and  $F_{2,n'}$  of the first and second samples, respectively, and  $I[X_i \leq x]$  is the indicator function equal to 1 if  $X_i \leq x$ , or 0 otherwise. In K-S tests, factor  $D_{n,n'}$  represents the maximum vertical distance between the CDF curves of two comparable vectors (herein FRF amplitudes for the helicopter NGB and the test rig). KS Similarity factors between the FRF vectors were derived by subtracting  $D_{n,n'}$  from unity.

## Results for Spiral Bevel Gear Fatigue Rig Under Static Conditions

The first part of the analysis was to characterize the test rig under static conditions. FRF measurements were made under different conditions to compare transfer paths from the gear/pinion tooth mesh to the accelerometers on the housing. For these tests, impacts were made at the gear mesh on the left pinion, and the response of the MSPU and MDSS accelerometers on the right and left side of the test rig were compared. The impacts at the gear mesh with the hammer were made on the pinion gear tooth in the vertical direction, as shown in Figure 7. This impact orientation was selected since the largest tooth force at the mesh was calculated for this direction.

### Varying Loads

The effects of loads on the transfer path were examined by impacting the hammer on the left pinion in the vertical direction and measuring its response with the MDSS system accelerometers. Accelerations were measured with the HF accelerometers from 0 to 6400 Hz. The test gears were loaded by applying a static torque in the loop. Four design loads were applied and are listed in Table 2. Similarity factors were then calculated comparing the 29 percent design load to the other three loads and are listed in Table 2. According to Table 2, similarity factors above 0.9 indicated the FRFs were similar under varying loads. Representative plots of FRF, Coherence and CDF at 104 percent design load compared to 29 percent load are shown in Figure 8.

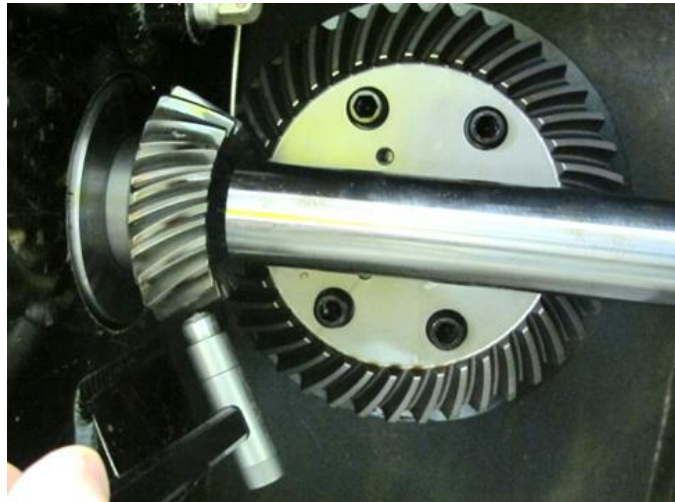


Figure 7.—Impact on left pinion in the vertical direction.

TABLE 2.—KOLMOGOROV-SMIRNOV (KS) SIMILARITY TESTS FOR FRFS AT 3 LOADS COMPARED TO 29 PERCENT LOAD

Percent design load	Gear torque, in.-lb	Pinion torque, in.-lb	KS similarity factor
29	2347	1088	na
53	4264	1976	0.91
78	6252	2897	0.90
104	8283	3838	0.92

These plots were also generated for a narrow frequency band (1800 to 3000 Hz) around the gear mesh and its sidebands for 3500 rpm gear speed (Table 1). This expanded scale is highlighted in yellow in Figure 8. Similarity factors calculated comparing the 29 percent design load to the other three loads are listed in Table 3. According to Table 3, similarity factors calculated for the narrow band were lower than the full range and decreased with an increase in load. Plots of FRF, Coherence and CDF at the three loads compared to 29 percent design load are shown in Figure 9. These results indicate that for the most accurate system structural characterization, loads similar to the operating loads should be applied during transfer path measurements. Further discussion of results will focus on measurements taken at the load closest to operating load under dynamic conditions. This load is highlighted in Table 3.

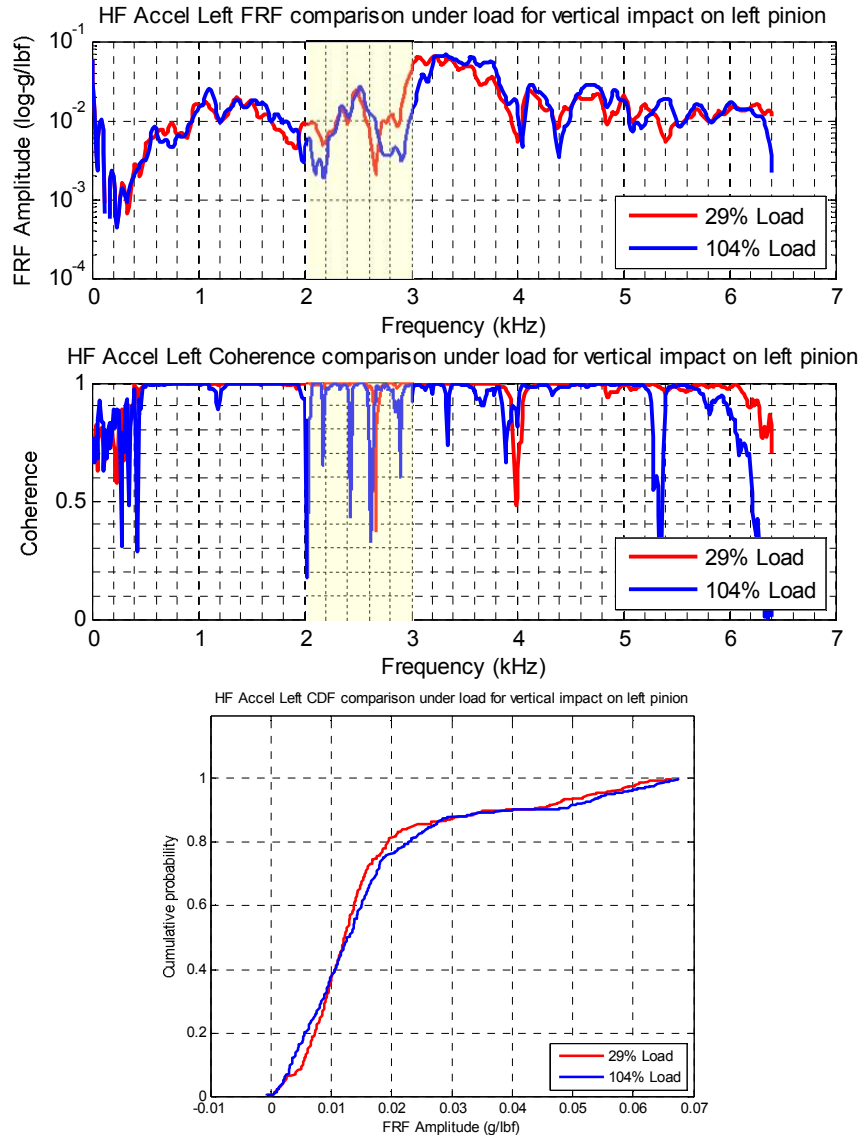


Figure 8.—FRF, Coherence and CDF at 104 percent design load compared to 29 percent load.

TABLE 3.—KS SIMILARITY TESTS FOR FRFS AT 3 LOADS COMPARED TO 29 PERCENT LOAD WITHIN A FREQUENCY BAND

Percent design load	Gear torque, in.-lb	Pinion torque, in.-lb	KS similarity factor
29	2347	1088	na
53	4264	1976	0.74
78	6252	2897	0.71
104	8283	3838	0.70

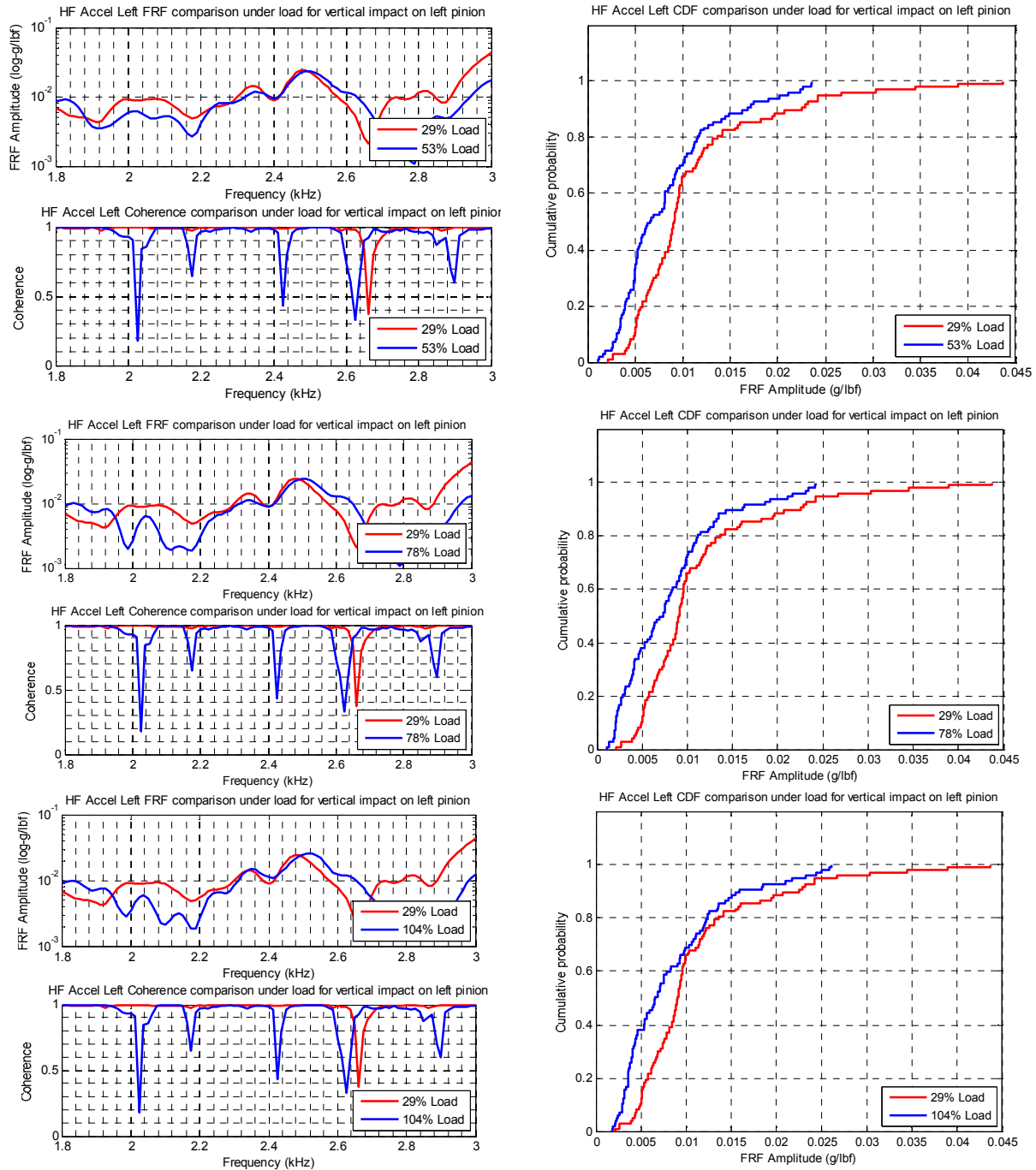


Figure 9.—FRF, Coherence and CDF at 53, 78, and 104 percent loads compared to 29 percent load.

## Coupling Between Left and Right Pinion

The test rig was designed to test two sets of spiral bevel gears simultaneously with the right and left pinions connected by a cross shaft. This design can make it more challenging to isolate tooth damage on one side of the gearbox from the other side. To investigate how damage on one side can potentially affect the other, impacts were made at the left pinion at 104 percent load and measured on the right and left side accelerometers. Figure 10 shows plots of FRF, Coherence and CDF at 104 percent load measured with the MDSS HF accelerometers on right and left sides of the gearbox. A KS similarity value of 0.65 was calculated for the 0 to 6400 Hz frequency range. The FRF amplitude measured on the left side was higher

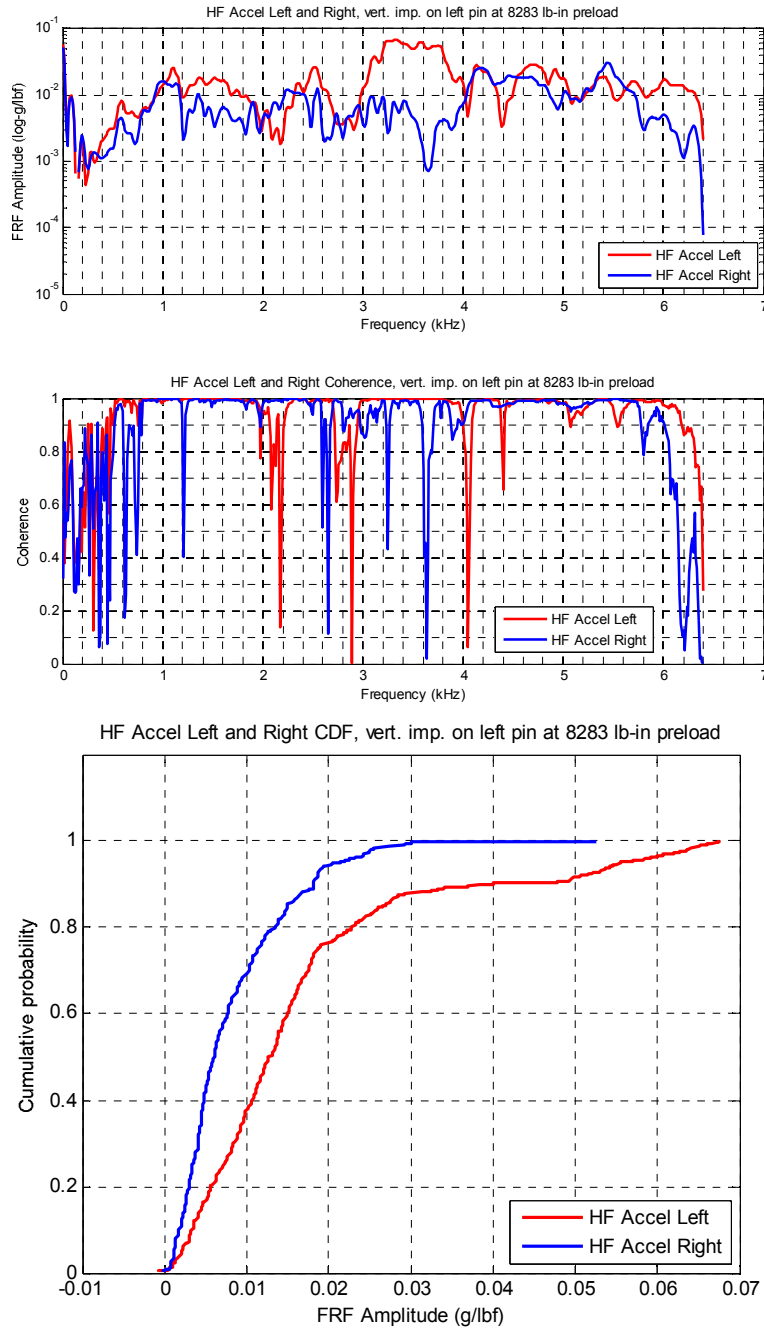


Figure 10.—FRF, Coherence and CDF at 104 percent load measured on right and left with HF accels.

than that of the right side due to impacts made closer to this accelerometer. The coherence for the left accelerometer seems better than in the right one across the entire frequency range, which seems reasonable since the location of the impact is closer to the left accelerometer. However, the right accelerometer did respond to this impact indicating the coupling between the right and left pinion through the shaft. The frequency bands from 2.6 to 4.0 kHz and the frequency after 5.4 kHz show big differences in amplitudes between the left and right accelerometers. The resonant frequency appears to be at 3.2 kHz. This is good news because it does not correlate to frequencies used for diagnostic purposes at 100 percent operating conditions of the test rig.

### Comparison Between MDSS and MSPU Accelerometers

Both the HF and Dytran accelerometers will be used during test rig failure progression tests. Dytran accelerometers used to monitor the helicopter NGB have an integral mounting bracket. To compare both types of sensors, impacts were made at the left pinion at 104 percent load and measured with the HF and Dytran accelerometers installed on the left side of the test rig gearbox. Figure 11 shows plots of FRF, Coherence and CDF at 104 percent load measured with both accelerometers. A KS similarity value of 0.94 was calculated for the 0 to 6400 Hz frequency range and 0.85 for the 1800 to 3000 Hz frequency range. This indicates both types of accelerometers respond within the frequency of interest.

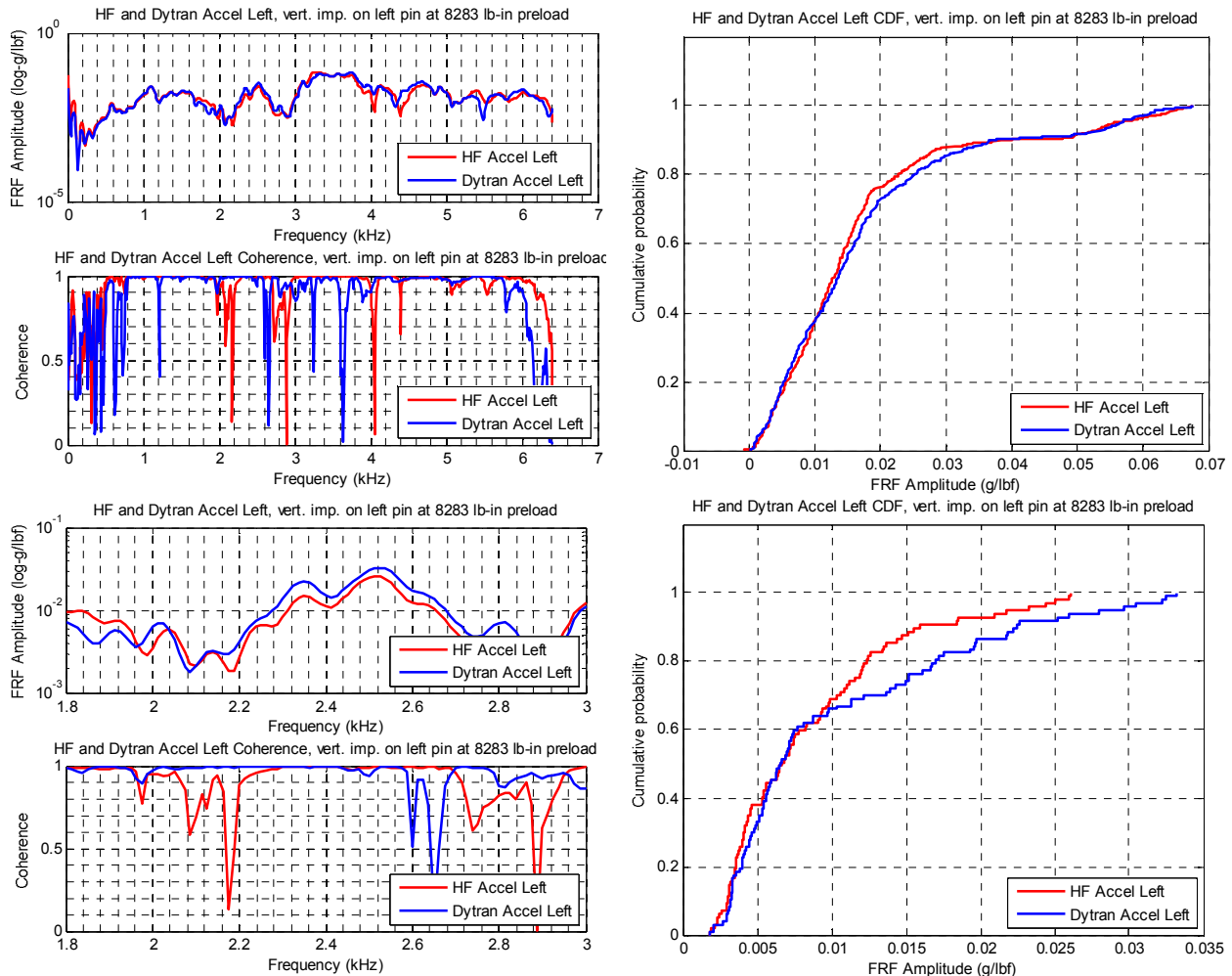


Figure 11.—FRF, Coherence and CDF at 104 percent load measured with HF and Dytran accels.

## Dynamic Response

One underlying objective of the FRF measurements was to determine if measuring the behavior of the structure under static conditions can provide any insight into CI performance under dynamic conditions. Dynamic data were collected on two different gear sets (pinion/gear), referred to as L3030R5050 and L1515R5050, installed on the left side of the test rig. The right gear set was not changed during the tests. Comparable oil temperatures and oil jet pressures were maintained for each test. Table 4 lists the operating speeds and loads during the dynamic tests.

The first gear set, referred to as L3030R505, completed 100 hours of operation before measurements were taken in support of this research. Damage occurred during the previous 100 hours of testing prior to performing these dynamic tests. Figure 12 is a photograph of the damage observed on the gear and pinion teeth. Figure 13 shows plots of the gear speed, gear mesh frequency and torque during the test. The gear speed in rpm and gear mesh frequency in Hz is plotted on the left y-axis. The torque is plotted on the right y-axis.

TABLE 4.—DYNAMIC TEST CONDITIONS

L3030R5050				L1515R5050				L1515R5050-2			
RPM	Hz	GM(Hz)	Torque	RPM	Hz	GM(Hz)	Torque	RPM	Hz	GM(Hz)	Torque
2000	33	1367	100%					2000	33	1367	100%
2500	42	1708	100%	2500	42	1708	100%	2500	42	1708	100%
3500	58	2392	100%	3500	58	2392	100%	3500	58	2392	100%
3000	50	2050	100%					3000	50	2050	100%
								2000	33	1367	29%
								2500	42	1708	29%
								3000	50	2050	29%
								3500	58	2392	29%

L3030R5050 – after 100 hours  
Damage to left gear and pinion teeth

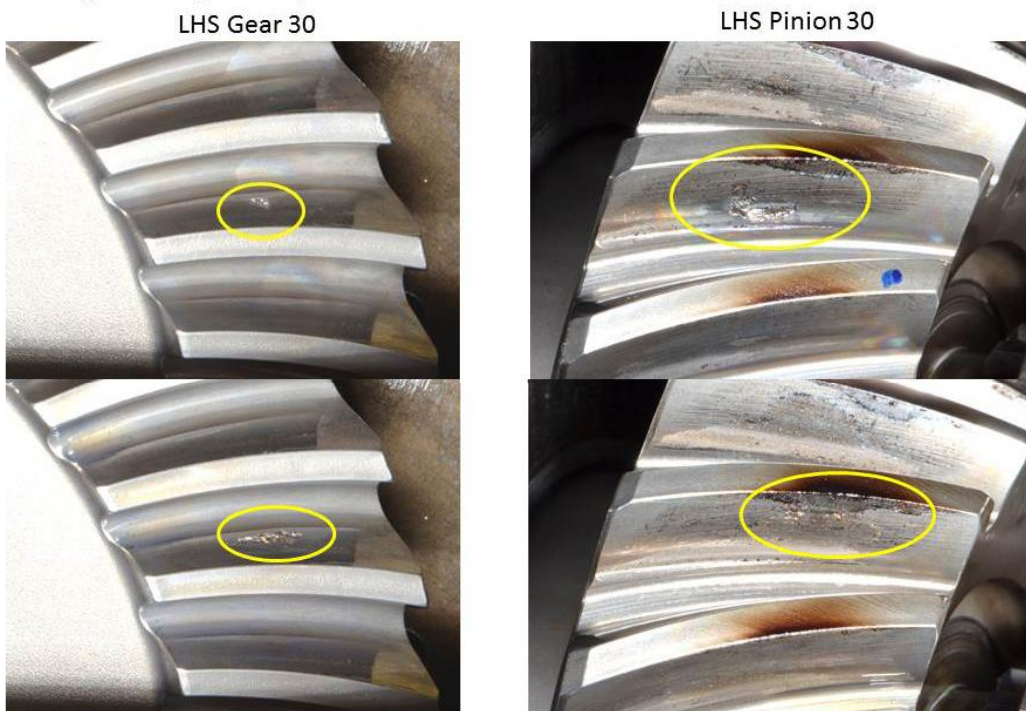


Figure 12.—Damage to gear and pinion teeth.

A snapshot of the TSA data and the corresponding spectrum data was plotted for each test condition. The yellow triangles on the x-axis of Figure 13 indicate points where the TSA data were plotted. The TSA time domain data were converted into the frequency domain using FFT. An example of plots of the TSA and the spectrum data for a point on the left pinion is also shown in Figure 13. The interpolated TSA data were averaged to one shaft revolution. The x-axis is the interpolated points of 1 revolution. The y-axis is in volts. The spectrum data plotted is the spectrum of the TSA. The x-axis is in shaft orders. For example, since the gear has 41 teeth, the gear mesh frequency (teeth x rpm) shows up at 41 shaft orders. The pinion shows up at 19 shaft orders due to 19 pinion teeth. The y-axis is in G-scale.

The second gear set, referred to as L1515R5050, was installed new on the test rig. An anomaly, due to the manufacturing process, was present at the root of the gear teeth at the start of the testing. Figure 14 shows a photograph of the anomaly observed on the gear teeth.

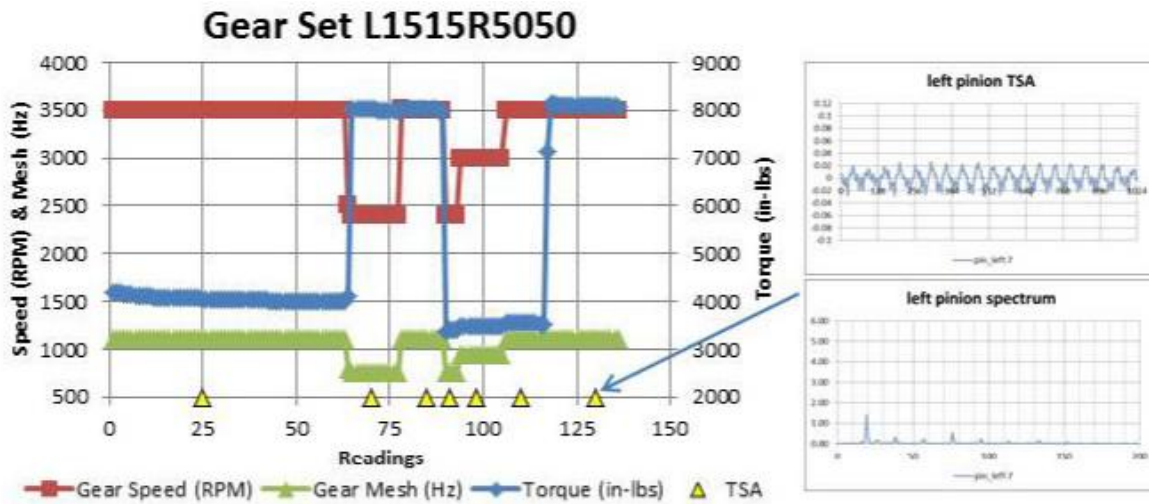


Figure 13.—Gear speed, gear mesh frequency and torque during L3030R5050 test.

### L1515R5050 – just installed

Surface anomaly on several left hand side gear # 15 teeth

#### LHS Gear 15



Figure 14.—Gear teeth anomaly on the second gear set.

Figure 15 shows plots of the gear speed, gear mesh frequency and torque during the test. The gear speed in rpm and gear mesh frequency in Hz is plotted on the left y-axis. The Torque is plotted on the right y-axis. A snapshot of the TSA data and the corresponding spectrum data was plotted for each test condition. The yellow triangles on the x-axis of Figure 15 indicate the point where the TSA data were collected. Note that the data used for this analysis were limited to points indicated by triangles 1, 3, 7 on the x-axis. The TSA time domain data were converted into the frequency domain using FFT.

The second gear set, referred to as L1515R5050, rotated for another 12 hr at 8000 in.-lb. Damage was observed on one pinion tooth at test completion. Figure 16 shows a photograph of the damage observed on the pinion teeth.

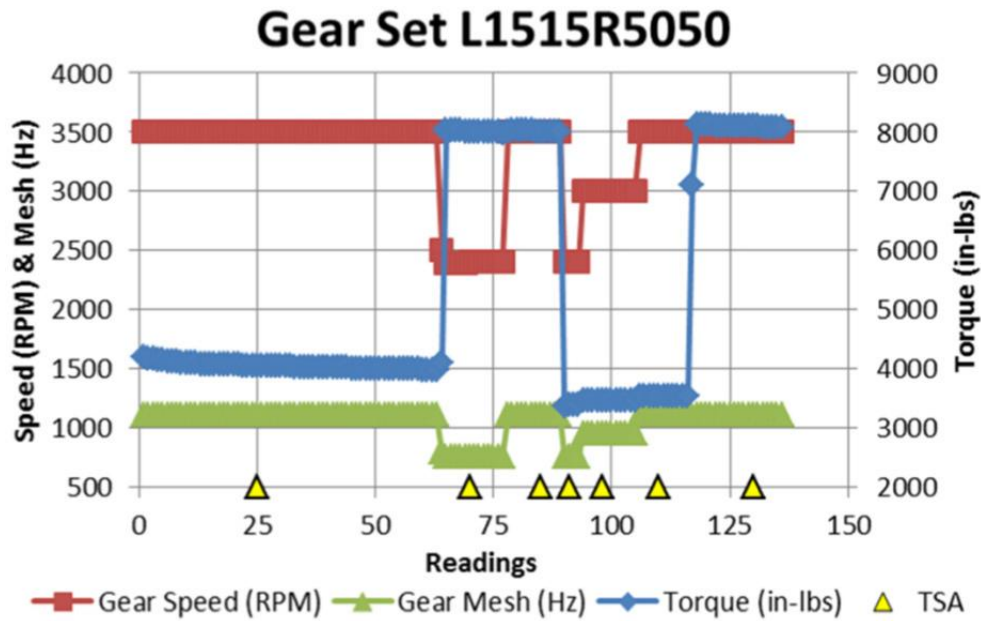


Figure 15.—Gear speed, gear mesh frequency and torque during L1515R5050 test.

L1515R5050 – after 12 hours of testing.

Damage to one left pinion tooth prior to collecting this data.

LHS Pinion 15



Figure 16.—Damage to one pinion tooth.

Figure 17 shows plots of the gear speed, gear mesh frequency and torque during the test. The gear speed in rpm and gear mesh frequency in Hz is plotted on the left y-axis. The torque is plotted on the right y-axis. A snapshot of the TSA data and the corresponding spectrum data was plotted for each test condition. The yellow triangles on the x-axis of Figure 17 indicate the point where the TSA data were collected. The TSA time domain data were converted into the frequency domain by performing FFT.

The objective of this analysis was to compare the dynamic response of two different left gear sets (L3030R5050 and L1515R5050) at comparable torques and speeds. The vibration data presented were collected with the MDSS HF accelerometers mounted on the right and left side of the rig gearbox. The average amplitude of the TSA data and amplitudes of the gear mesh frequencies and their harmonics were used to compare the differences in dynamic response. In the gear mesh amplitude tables, 1H indicates the first, 2H the second and 3H the third harmonic of the gear mesh. Note that only the left gear set was changed. The right set remained the same for all test conditions.

Tables 5 and 6 summarize the frequency domain response of the right and left gearbox accelerometers while Tables 7 and 8 summarize the time domain response of the accelerometers. The torque was maintained and speed varied. For the test condition noted by an asterisk in Tables 5 and 6, the test rig was shut down, inspected, and then data was taken again at the same condition. Tables 9 and 10 summarize time domain and frequency domain response of the left side of the gearbox at varying speeds and low torque on gear set (L1515R5050-2) with damage on one tooth.

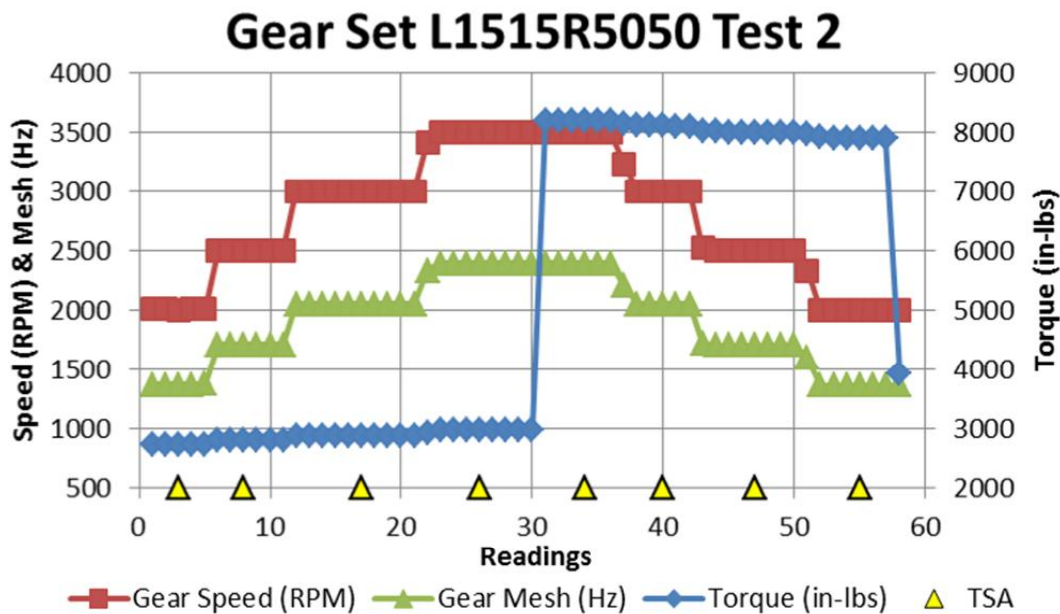


Figure 17.—Gear speed, gear mesh frequency and torque during L1515R5050-2 test with damage.

TABLE 5.—LEFT GEAR MESH AMPLITUDES AT HIGH TORQUE AND VARYING SPEED

Gear Mesh Amplitude					
RPM	Torque	L3030 Left	L1515 Left	L1515 Left	L1515-2 Left
2000	8000	1H=2.75			1H=1.5
2500	8000	1H=2H=1.7	1H=1, 2H=3		1H=4
3500	8000	1H=3	1H=1.5, 2H=1	*1H=1.5	1H=3, 2H=1.5
3000	8000	1H=5			1H=3

TABLE 6.—RIGHT GEAR MESH AMPLITUDES AT HIGH TORQUE AND VARYING SPEED

Gear Mesh Amplitude					
RPM	Torque	L3030 Right	L1515 Right	L1515 Right	L1515-2 Right
2000	8000	1H=2H=1.2			1H=5.5, 2H=1.75, 4H=3
2500	8000	1H=2.5, 2H=3.5	1H=.7, 2H=4.5		1H=8
3500	8000	1H=5	1H=5, 2H=1.5, 3H=2.5	*1H=6, 2H=2, 3H=3	1H=2.5, 2H=1
3000	8000	1H=6			1H=2H=3

TABLE 7.—LEFT TSA AMPLITUDES AT HIGH TORQUE AND VARYING SPEED

TSA Amplitude Left		Gear	Pinion	Gear	Pinion	Gear	Pinion	Gear	Pinion
RPM	Torque	L3030 Left	L3030 Left	L1515 Left	L1515 Left	L1515 Left	L1515 Left	L1515-2 Left	L1515-2 Left
2000	8000	$\pm 0.04$	$\pm 0.05$					$\pm 0.04$	$\pm 0.03$
2500	8000	+0.04-0.05	+0.05-0.07	$\pm 0.05$	$\pm 0.04$			+0.05-0.06	+0.04-0.06
3500	8000	$\pm 0.09$	$\pm 0.09$	$\pm 0.04$	$\pm 0.03$	+0.03-0.04	$\pm 0.03$	+0.05-0.04	+0.04-0.03
3000	8000	$\pm 0.08$	+0.1-0.08					$\pm 0.06$	$\pm 0.04$

TABLE 8.—RIGHT TSA AMPLITUDES AT HIGH TORQUE, VARYING SPEED

TSA Amplitude Right		Gear	Pinion	Gear	Pinion	Gear	Pinion	Gear	Pinion
RPM	Torque	L3030	L3030	L1515	L1515	L1515	L1515	L1515-2	L1515-2
2000	8000	+0.04-0.02	+0.04-0.02					$\pm 0.1$	$\pm 0.1$
2500	8000	$\pm 0.07$	+0.06-0.07	+0.06-0.07	$\pm 0.06$			$\pm 0.1$	$\pm 0.1$
3500	8000	$\pm 0.09$	$\pm 0.09$	$\pm 0.1$	$\pm 0.07$	+0.12-0.1	+0.12-0.1	$\pm 0.04$	$\pm 0.04$
3000	8000	+0.09-0.1	$\pm 0.08$					+0.08-0.06	+0.07-0.04

TABLE 9.—LEFT GEAR MESH AMPLITUDES AT LOW TORQUE AND VARYING SPEED

Gear Mesh Amplitude			
RPM	Torque	L1515-2 Left	L1515-2 Right
2000	2740	1H=0.5	1H=0.5
2500	2812	1H=1	1H=1
3000	2890	1H=1.5	1H=5
3500	2974	1H=1.2	1H=1.7

TABLE 10.—LEFT TSA AMPLITUDES AT LOW TORQUE AND VARYING SPEED

TSA Amplitude		Gear	Pinion	Gear	Pinion
RPM	Torque	L1515-2 Left	L1515-2 Left	L1515-2 Right	L1515-2 Right
2000	2740	$\pm 0.01$	$\pm 0.01$	$\pm 0.01$	$\pm 0.01$
2500	2812	$\pm 0.02$	$\pm 0.02$	$\pm 0.02$	$\pm 0.02$
3000	2890	$\pm 0.02$	$\pm 0.02$	$\pm 0.06$	$\pm 0.06$
3500	2974	$\pm 0.02$	$\pm 0.02$	$\pm 0.04$	$\pm 0.02$

After review of the data, the following observations were made per the left side datasets:

1. For speeds 2000, 3000, and 3500 rpm, the first harmonic was the dominant frequency measured by the left accelerometer for both gear sets for all conditions.
2. For the speed of 2500 rpm (1708 Hz GM), the 2<sup>nd</sup> and 3<sup>rd</sup> harmonics were almost equal for gear set 30, and the 2<sup>nd</sup> harmonic was greater than the 1<sup>st</sup> for gear set 15. Due to the unusual dynamics at this speed, this speed should be avoided during testing.
3. The gear set 30, with the most damage during testing, had the highest amplitude in the time domain.

After reviewing the data, the following observations were made per the right side datasets:

1. For the speed of 3500 rpm, the first harmonic was the dominant frequency measured by the right accelerometer for both gear sets for all conditions.
2. For the speed of 2500 rpm, the 2<sup>nd</sup> harmonic was greater than the 1<sup>st</sup> harmonic for both gear sets. However, this changed for gear set 15 once damage occurred. Due to the unusual dynamics at this speed, this speed should be avoided during testing.
3. For speeds of 2000 and 3000 rpm, the dynamics changed for different operating conditions, where in two cases the 1<sup>st</sup> and 2<sup>nd</sup> harmonics were equal.
4. The highest TSA amplitude and gear mesh amplitude occurred on the right side at 3000 rpm.

Comparing torques to varying speeds, for gear set L1515R5050-2, the amplitudes of the gear mesh increased with higher torques for all speeds. The TSA increased with higher torques for all speeds except at 3500 rpm on the right gear. Further investigation is warranted to determine the cause of this response.

Accelerometer response changed with varying loads, speeds, gear sets and damage levels. Overall, the right side was more sensitive to changes in speed and load. Due to the environmental conditions affecting vibration response, isolating a relationship between structural FRF response and dynamic conditions was challenging for these datasets. The FRFs and coherence from Figure 10 are plotted in Figures 18 and 19 at 104 and 29 percent load with expanded scales of 0 to 1000 Hz and 1000 to 2000 Hz. The purpose was to determine if the FRFs at the frequencies tested would indicate the observed responses while the rig was rotating. Higher amplitude resonances were observed under low load conditions at lower frequencies possibly indicating the varying response at the lower speeds and loads. However, no unusual response near 2500 rpm (42 Hz) that corresponds to 1708 Hz GM was noted. But according to Figure 10, the resonant frequency appears to be at 3.2 kHz with a larger rise in amplitude between 3.4 and 3.8 kHz when compared to the response at other frequencies. The 2<sup>nd</sup> harmonic of gear mesh at 2500 rpm is equal to 3.4 kHz. The 2<sup>nd</sup> harmonic of the gear mesh for this speed was equal to or larger than the 1<sup>st</sup> for two of the gears tested.

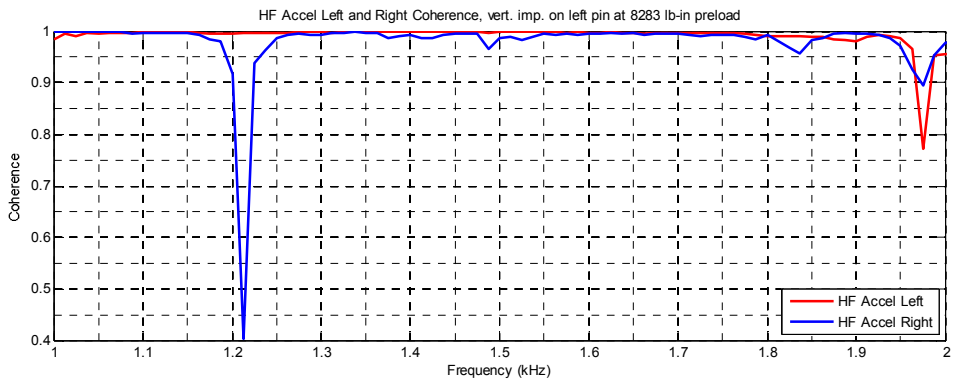
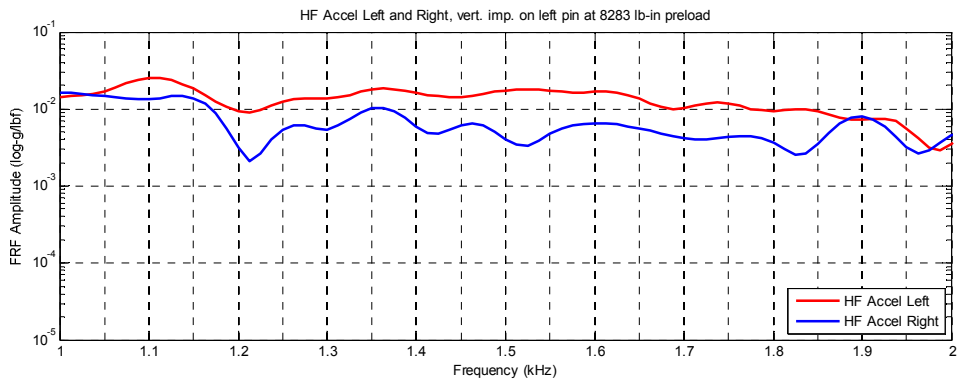
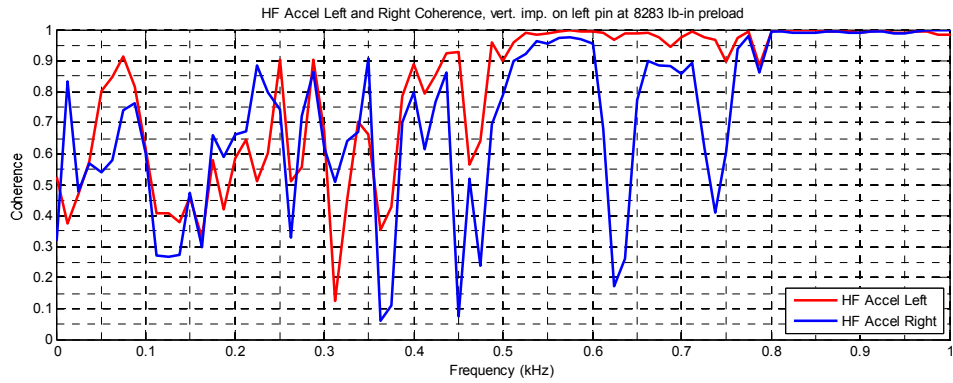
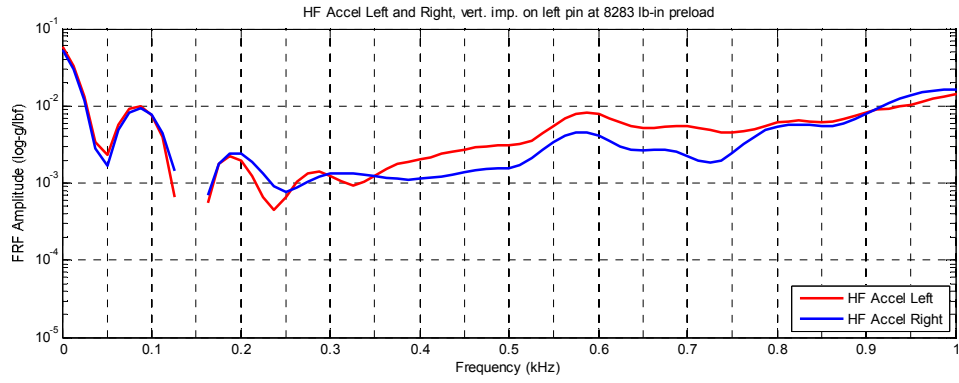


Figure 18.—FRF, Coherence and CDF at 104 percent load measured on right and left.

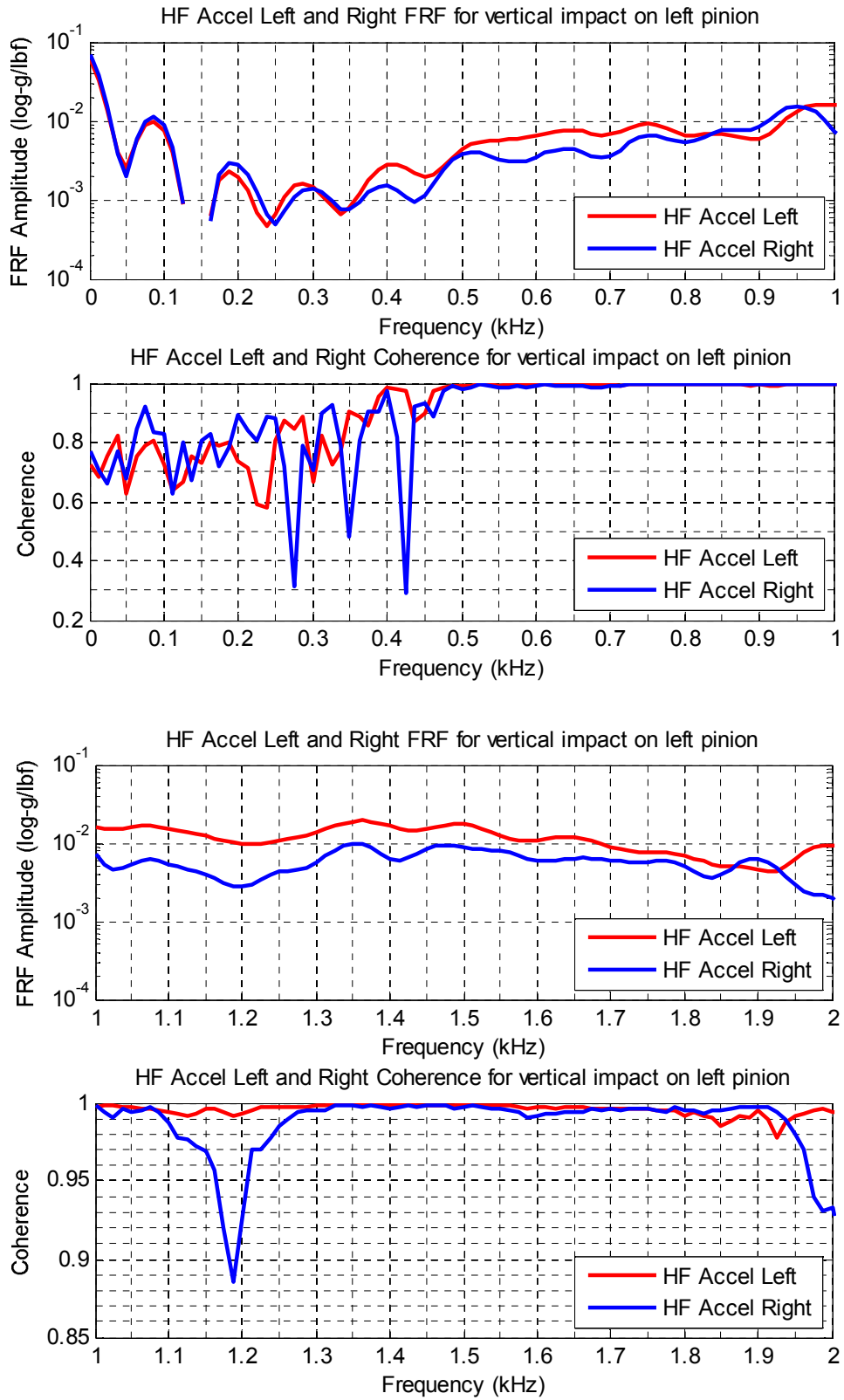


Figure 19.—FRF, Coherence and CDF at 29 percent load measured on right and left.

## Comparison of the Spiral Bevel Geared Systems

One objective of making FRF measurements on the test rig was to compare them to the NGB fixture and the helicopter NGB to determine if measuring the behavior of the structure under static conditions can provide any insight into CI performance between the helicopter and test rig. Measurements were made in the NGB fixture with the actuator on the ring gear and compared to measurements made with the actuator installed on the ring gear within the test rig banded around each system's gear mesh frequencies at specific torques.

FRFs and coherence were measured with the Dytran accelerometer with the shaker on the ring gear, at a frequency band that contains  $\pm 3$  sidebands around the gear mesh. These measurements were taken at 20 and 107 percent load conditions. These plots and the corresponding CDF plots are shown in Figure 20. The KS Similarity factor within this narrow frequency band between these two loads was equal to 0.68. The coherence improved at the higher load. The shape of the FRF signature changed at the higher load illustrating the importance of assessing the similarities of frequency response within frequencies of interest.

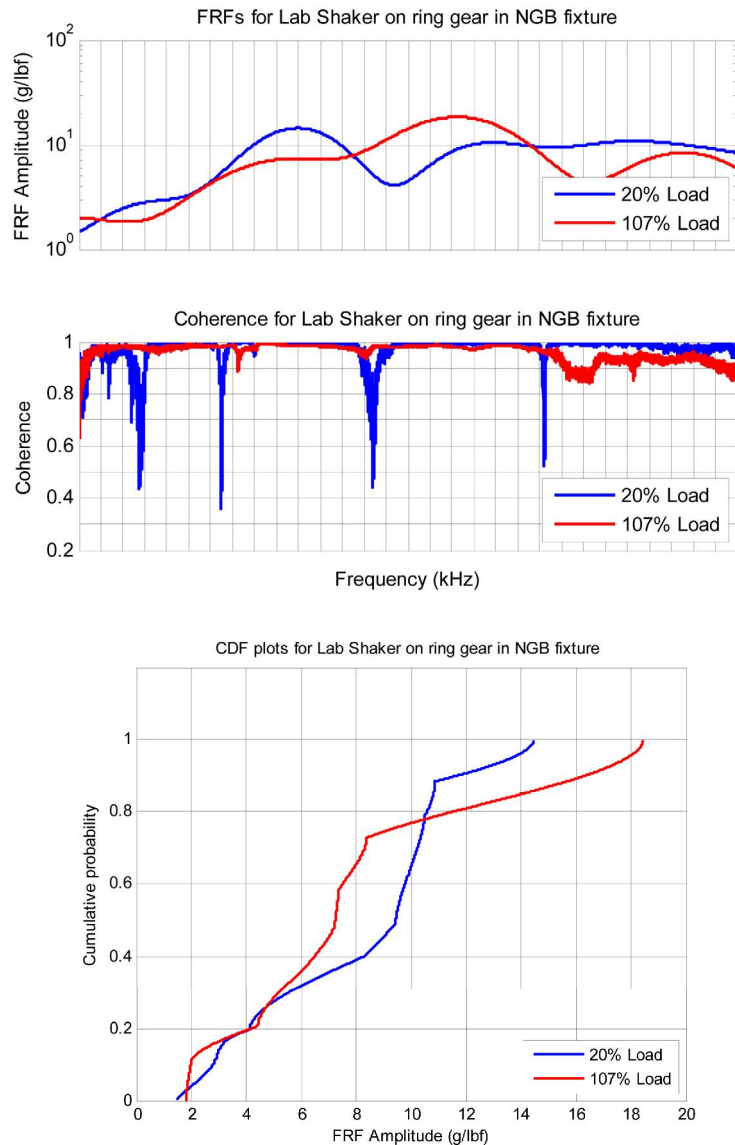


Figure 20.—HUMS FRFs, Coherence and CDF at 20 and 104 percent loads.

The frequencies of interests are different between the test rig and the helicopter requiring different methods of impact to obtain the 1.8 to 3 kHz versus the helicopter frequency band. It is important to understand how each system structure affects the response of the CI under its operating conditions. The most comparable measurement taken on both systems was the installation of an actuator on the ring gear and measuring the vibration response at the housing. This type of measurement is poor at the lower frequencies of interest for the test rig, due to the low energy of the reaction-mass shaker at low frequency. Figure 21 is a photograph of the piezoelectric actuator installed on the test rig gear and the NGB fixture. The vibration response on the NGB fixture was measured with a high frequency accelerometer with specifications comparable to the test rig HF accelerometers, mounted in the horizontal position. The vibration response on the test rig was measured with the HF accelerometers mounted in the vertical position on the external housing. The gearbox housings are very different, as shown in Figure 2, indicating the vibration transfer paths between the NGB fixture and the test rig would also be different.

The measurements on the NGB fixture were taken at 4 percent load, while the measurements on the test rig were taken at 46 percent load. The 4 percent load was used for the NGB fixture because these measurements can only be taken at that load. FRFs, coherence and the corresponding CDF plots are shown in Figure 22. The KS Similarity factor for 0 to 50 kHz was equal to 0.25, which indicates very different vibration transfer paths between the two structures. This is no surprise based on the design of the two systems. One interesting observation is that the FRF amplitude is significantly higher on the helicopter indicating the helicopter may be more responsive to gear fault signatures than the test rig. This observation suggests that the helicopter gearbox may generate higher noise that could potentially mask vibration amplitude changes due to faults.

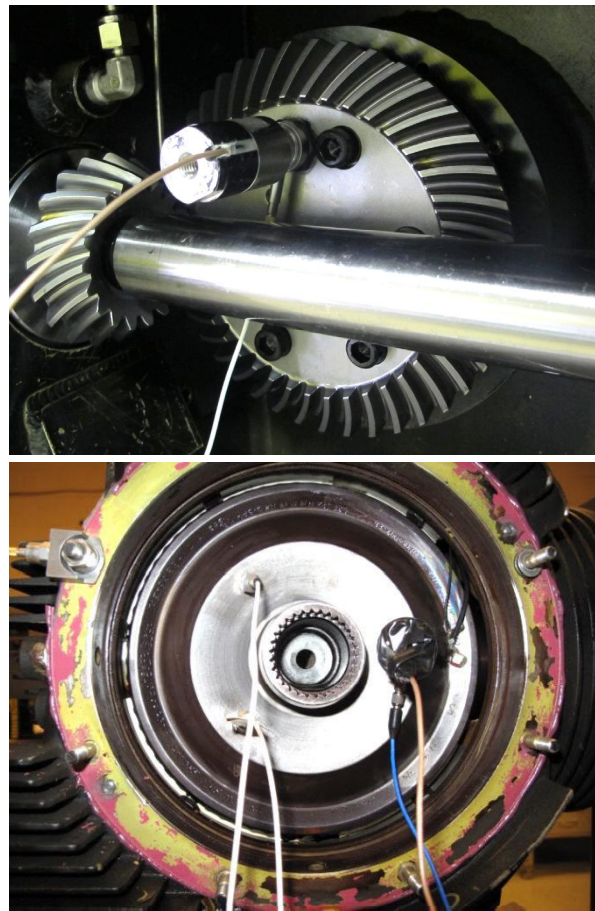


Figure 21.—Actuators installed on the test rig and NGB fixture.

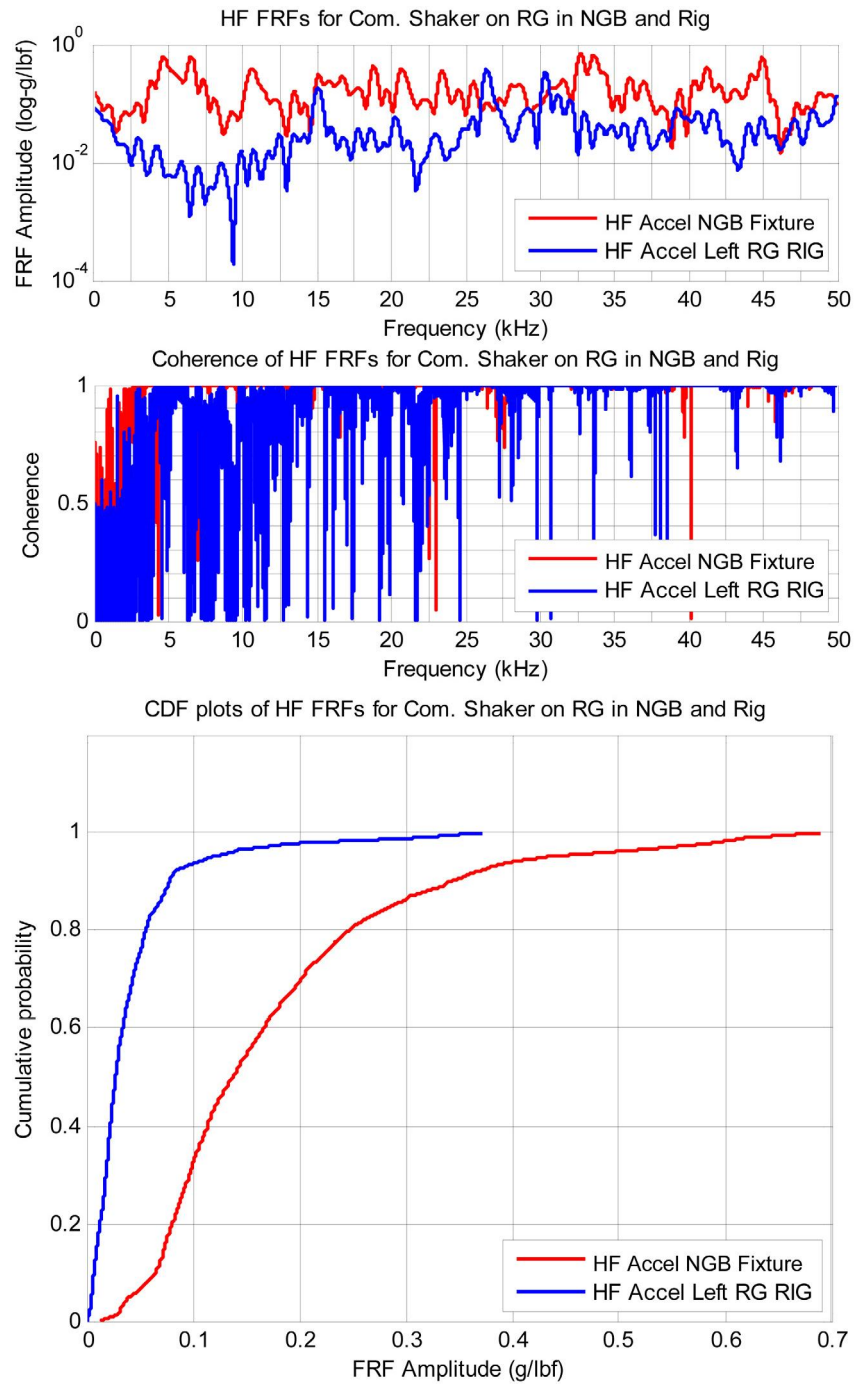


Figure 22.—FRFs, Coherence and CDF of test rig and NGB fixture.

## Summary

Transfer path measurements taken on the test rig to assess the utility of static vibration transfer paths in assessing dynamic gear CI performance provided some insight into gear condition indicator performance. Varying load affected the transfer paths within specific frequency bands used for gear condition indicators. The unique design of the test rig caused a coupling between the right and left gearbox through the shaft indicating difficulties in isolating pinion tooth damage on one side of the gearbox. Both the high frequency and the helicopter accelerometers responded similarly to the same impact indicating both can be used for CI development. Measuring the dynamic behavior of the structure in specific frequency bands under static conditions using frequency response functions (FRF) provided limited insight into spiral bevel gear CI performance under dynamic conditions. The amplitude of the gear mesh and TSA values increased with higher torques. A resonance near gear mesh under static conditions caused unusual dynamic response when operated at this frequency. The comparison of the FRFs between the helicopter NGB and the test rig was challenging since the frequencies of interest are different for both systems and measurements were not taken under comparable loads. However, one interesting observation was that the FRF amplitude measured on the helicopter NGB was significantly higher than that measured on the test rig indicating the helicopter may be more responsive to gear faults. Based on these analyses, although some useful information can be gleaned and perceived from static transfer path measurements, the system structure, such as test rig, helicopter NGB, NGB fixture does not significantly affect the vibration response of an accelerometer to the dynamic gear mesh signatures. It is more important to understand the dynamic characteristics unique to each system to be used for CI development that affect individual gear CI response for a healthy and damaged tooth.

## References

1. Dempsey, P.J., Brandon, E.B., "Validation of Helicopter Gear Condition Indicators Using Seeded Fault Tests," NASA/TM—2013-217872, April 2013.
2. Antolick, L.J., Branning, J.S., Wade, D.R., and Dempsey, P.J., "Evaluation of Gear Condition Indicator Performance on Rotorcraft Fleet," American Helicopter Society 66<sup>th</sup> Annual Forum Proceedings, Phoenix, Arizona, May 11-13, 2010.
3. Delgado, I.R., Dempsey, P.J., Antolick, L.J., and Wade, D.R., "Continued Evaluation of Gear Condition Indicator Performance on Rotorcraft Fleet," American Helicopter Society Condition Based Maintenance Specialist Meeting, February 2013.
4. Islam, A., Dempsey, P., Feldman, J. and Larsen, C., "Characterization and Comparison of Vibration Transfer Paths in a Helicopter Gearbox and a Fixture Mounted Gearbox." NASA TM-216586, September 2013.
5. Handschuh, R.F.: Thermal Behavior of Spiral Bevel Gears. NASA TM-106518, 1995.
6. Handschuh, R.F.: Testing of Face-Milled Spiral Bevel Gears at High-Speed and Load. NASA/TM—2001-210743, 2001.
7. Stewart, R.M. 1977. Some useful data analysis techniques for gearbox diagnostics. Machine Health Monitoring Group, Institute of Sound and Vibration Research, University of Southampton, Report MHM/R/10/77, July 1977.
8. Zakrajsek, J.J. 1989. An investigation of gear mesh failure prediction techniques. NASA TM-102340, AVSCOM TM 89-C-005.
9. Massey, F.J. "The Kolmogorov-Smirnov Test for Goodness of Fit." Journal of the American Statistical Association. vol. 46, no. 253, 1951, pp. 68-78.



